ISSN No:-2456-2165

Experimental Analysis of Aluminium Alloy Reinforced with Rare Earth Metals

Parasa Rajesh[1]; B.P. Maddiletty[2]; Dr. P. Ravikanth Raju[3]
Anurag University

Abstract:- Metallurgy is the science and technology of metals and alloys. It involves the production of metals by processing the ores to extract the metal they contain, and the mixing of metals or other elements to produce alloys. metals generally exhibit very particular properties; these properties are often limited to a very narrow field of application. The art of the metallurgist is to create alloys from a given base metal, like aluminium, copper, iron, etc. by adding controlled proportions of other metals or metalloids to improve or modify certain properties such as mechanical properties, formability, weldability. Aluminium is an extremely versatile metal and can be cast, melted, formed, machined, and extruded with several advantages, it is recognised for being lightweight, flexible, high specific strength, high processability, anti-erosion, increased conductivity, eco-friendly nature, and recoverability. Its applications are further widened by the preparation of alloys. Aluminium alloys are widely used in the fields of electric module packaging, automotive body structure, wind, and solar energy management. All aluminium products belong to one of eight alloy series.

The Rare earth metals (RE) offer a possibility to bond metal powders and their uses in metallic catalysts are growing. Alloys containing large quantities of RE are useful in high vacuum systems for removing H, CH and Ar. And used in incendiary applications on account of their superior pyrophoric properties. Addition of Res to Al offers heat resistance and better ductility. Hence in this project RE are experimentally added to the selected Al alloy in calculated proportions to produce the metal with extraordinary properties and contribute to the field of add an appropriate use here.

Keywords:- *Aluminium, Cerium, Conventional Stir Casting, Rare Earth Metal.*

I. INTRODUCTION

Composite material is a material composed of two or more distinct phases (matrix phase and reinforcing phase) and having bulk properties significantly different from those of any of the constituent material properties. Many of common materials (metals, alloys, doped ceramics and polymers mixed with additives) also have a small number of dispersed phases in their structures, however they are not considered as composite materials since their properties are similar to those of their base constituents (for example, physical property of steel is similar to those of pure iron). Favourable properties of composites materials are low density, high temperature stability, high stiffness and high strength, high electrical and thermal conductivity, corrosion resistance, improved wear resistance adjustable coefficient of thermal expansion, etc.

Properties of composite material can be considered under two headings those that depend solely upon the geometrical arrangement of the phases and their respective volume fractions and not at all upon the dimensions of the components and those depend on structural arrangements such as periodicity of arrangements or the sizes of the pieces of the two or more component phases. Indeed, in many instances the properties of phases making the composite start changing when the smallest dimension of the phase falls below a certain dimension. it is seen that the mechanical properties of metal matrix composites are dependent on the type and volume fraction of the reinforcement, dislocation strengthening and the defects introduced during the fabrication of MMCs. Most widely considered property in MMCs are its tensile strength, ductility, hardness and fracture.

Development and modification of aluminium alloys for industrial applications is a never-ending process. Aluminium alloys play an important role in the development of aerospace, defence, and automotive industry due to their improved mechanical properties as well as their low weights. While 2XXX series Al alloys in which copper is the principal alloying element and 7XXX series in which zinc is the principal alloying element are at the forefront of defence and aerospace industry, 6XXX series Al alloys containing Mg and Si are used for architectural extrusions and automotive components.

Al-2024 aluminium alloy has good machinability, high strength and fatigue resistance. Because of that, it is widely used in aircraft structures, gears and shafts, missile parts, orthopaedic equipment and scientific instruments. Al-6082 is known as a structural alloy and has medium strength and good corrosion resistance. This alloy is used for cranes, highly stressed applications, ore skips, bridges, and transport applications. General characteristics of Al-7075 alloy are very high strength comparable to many steels, good fatigue strength, average machinability but less resistance to corrosion than many other aluminium alloys.

Industrial development of aluminium-based alloys is conservative because it is mostly concentrated on modifications of common and well-known alloy systems (Al-Cu, Al-Si, Al-Mg-Si, Al-Zn-Mg, AlLi-Cu, etc.) and processing routes. The reason is that there is a lack of experience in new alloy systems and production methods. However, standard systems stated above seem to approach their mechanical limits.

ISSN No:-2456-2165

Rapidly solidified (RS) alloys of non-conventional compositions recently attracted great interest, because they are able to achieve tensile strength exceeding 1000 MPa. In particular, RS Al-TM-based alloys (TM=transition metals, such as Fe, Ni, Cr, V, Zr, Ti, rare earth metals, etc.) with amorphous or nanocrystalline structure are of importance. The Rare earth elements (REE), including scandium (Sc), yttrium (Y) and 14 lanthanides, belong to group IIIB of the periodic table of the elements. Because of their rare and unique physicochemical, magnetic and optical properties, REEs hold great potential for various industrial applications like compact fluorescent and LED lights, automatic catalytic converters, high-performance magnets, superconductors, catalysis, resonance imaging machines, electric vehicle batteries, high strength alloys, and lightweight aircraft component.

The rare earths or rare-earth elements (REEs) are a group of 17 chemically similar metallic elements (15 lanthanides, plus scandium and yttrium). They are becoming increasingly important in the transition to a green, low-carbon economy. This is due to their essential role in permanent magnets, lamp phosphors, rechargeable NiMH batteries, catalysts and other applications. Aluminium 2024 alloy is vastly used in transportation industry due to its high strength and low density.

II. MATERIALS AND METHODS

A. Material Composition

Commercial grade Aluminium alloy 2024 billets and Cerium particulates were obtained from the market. The specifications/composition obtained are presented below.

➢ *Aluminium Alloy 2024:*

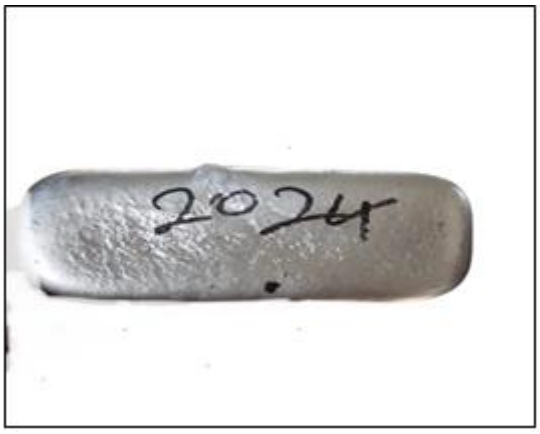

Fig 1 Al 2024

Fig 2 Cerium

- Si: 0.4-0.8 %max
- Fe: 0.7 %max
- Cu: 0.15-0.40 %
- Mn: 0.15 %max
- Mg: 0.8-1.2 %
- Cr: 0.4-0.35 %
- Zn: 0.25 %max
- Ti: 0.15 %max

- Cerium particles: 0.1g - 0.3g

B. Experimental Process:

The experimental procedure that has been followed is described below.

- The aluminum alloy 2024 is heated at 750°C, then 0.1g of cerium is added to aluminum alloy using the method of stir casting process.
- Then the molten metal alloy is poured into the dies and after cooling the test samples are obtained. The obtained test sample is of the composition (1920g Al2024 + 0.1g Cerium).
- Again, repeating with the same process test samples (1940g Al2024 + 0.2g Cerium) and (1960g Al2024 + 0.3g Cerium) are also obtained.
- After the preparation of the test samples, the internal stresses are removed by heat treatment to ensure the accuracy of the test results.
- Further the test samples are tested for its hardness, compression and tensile strengths.
- Finally, the results obtained are discussed and analyzed as mentioned below.

Table 1 Combustion Properties of Hydrogen, Methane, and Gasoline

Properties	Hydrogen	Methane	Gasoline
Limits of flammability in air (vol %)	4.0–75.0 29.53	5.3–15.0	1.0–7.6
Stoichiometric composition in air (vol %)	0.02	9.48	1.76
Minimum energy for ignition in air (mJ)	858	0.29	0.24
Auto-ignition temperature (K)	2318	813	501–744 2470
Flame temperature in air (K)	265–325	2148	37–43
Burning velocity in NTP air (cm s^{-1})	0.064	37–45 0.203	0.2
Quenching gap in NTP air (cm)	17–25	23–32	30–42

Percentage of thermal energy radiated from flame to surrounding (%)	0.63	0.2	0.08
Diffusivity in air (cm2 s^{-1})	1.00	1.7	1.7
Normalized flame emissivity (2000 K, 1 atm)	0.1–7.1	0.53–1.7	0.7–3.8
Limits of flammability (equivalence ratio)			

Exhaustive tests by researchers in the Indian Institute of Technology (IIT) Delhi in the laboratory have shown that it is possible to operate a hydrogen engine that is capable of ultra lean operation thereby producing extremely low levels of NO_x emissions. Compression ignition (CI) of hydrogen is extremely difficult because of hydrogen's auto-ignition temperature and therefore a hydrogen-operated diesel cycle is not easily achievable.

At the same time, this property of high self-ignition temperature can be very useful to a spark ignition (SI) engine in which the compression ratio can be substantially increased, thereby increasing the thermal efficiency. After a critical review of some of the properties of hydrogen, it is clear that an optimal hydrogen engine can be designed on the basis of unique properties of hydrogen so as to have a much higher thermal efficiency and substantially lower exhaust emission as compared with the existing conventional gasoline engine.

III. RESULTS AND DISCUSSION

The first step in the study of any newly prepared sample, is the study of its microstructure/grain structure. Since the arrangement of the molecules plays an important role in defining the physical and chemical properties, the study of microstructure is significant. The microstructure/grain structure of three different test samples of varying composition of Al2024 and Cerium (namely, 1920g Al2024 + 0.1g Cerium, 1940g Al2024 + 0.2g Cerium and 1960g Al2024 + 0.3g Cerium) were obtained using Optical Metallurgical Microscope (Model No. MET SCOPE-I) and observed microstructures were as given below.

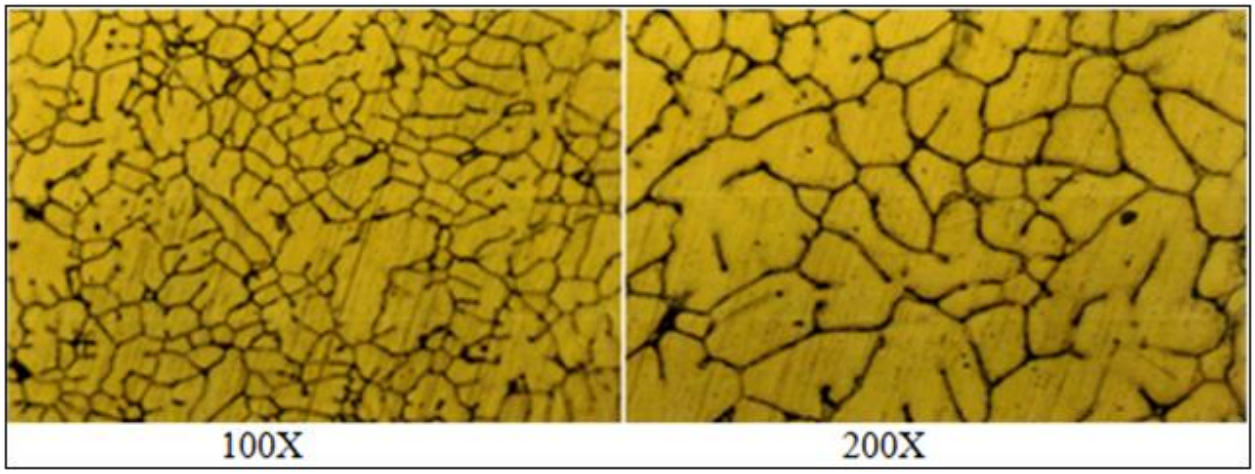

Fig 3 Microstructure of (1920g Al2024 + 0.1g Cerium)

The microstructure consists of strip like, distributed along the grain boundaries while some granular phases were also found in the inner grains. Neither micro porosities nor stringers were observed.

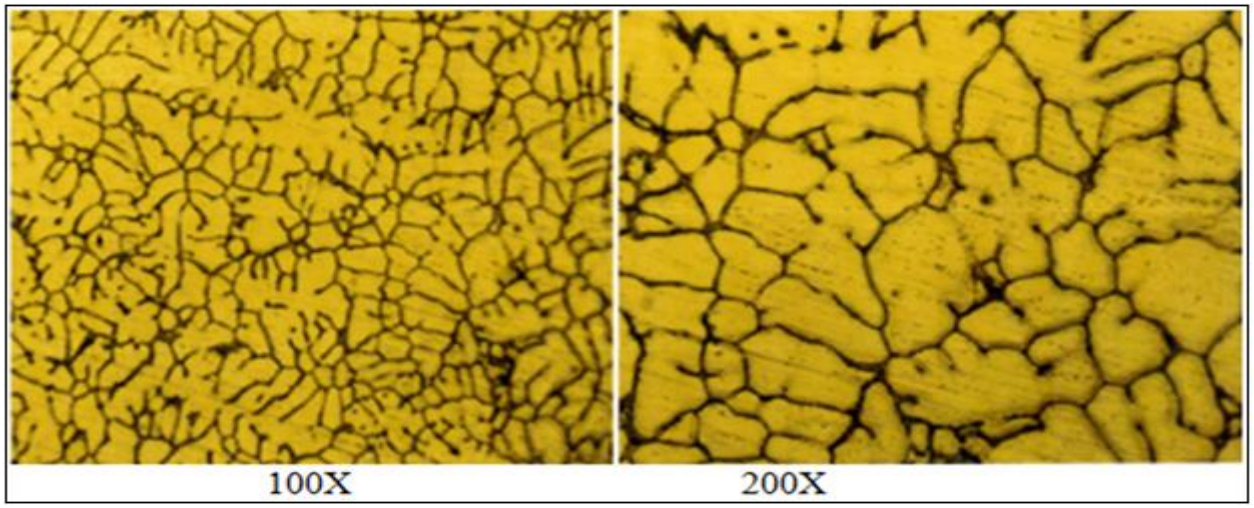

Fig 4 Microstructure of (1940g Al2024 + 0.2g Cerium)

ISSN No:-2456-2165

The microstructure consists of strip like, distributed along the grain boundaries while some granular phases were also found in the inner grains. Neither micro porosities nor stringers were observed.

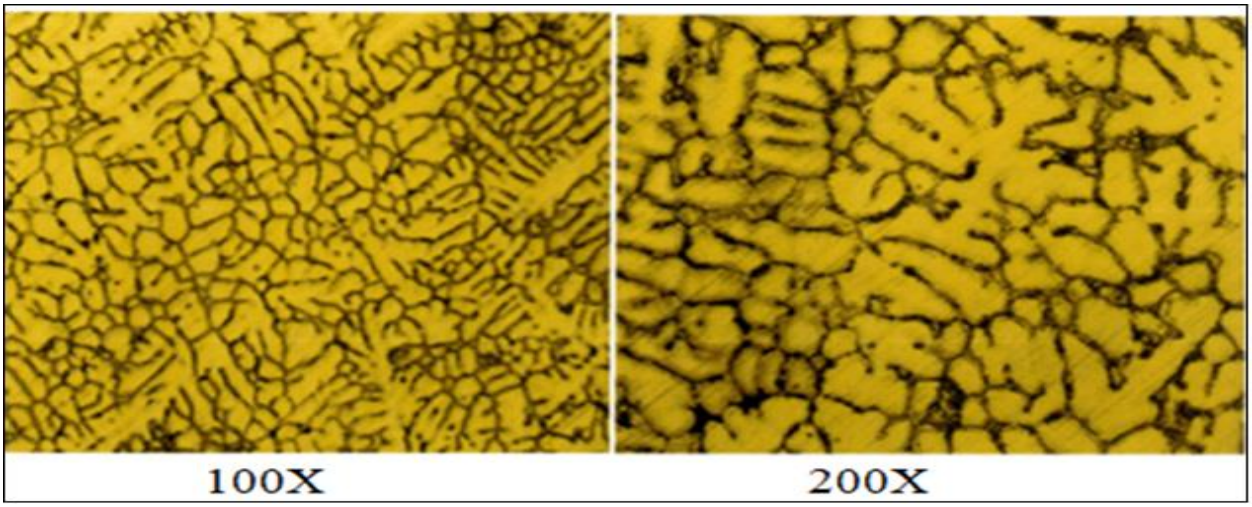

Fig 5 Microstructure of (1960g Al2024 + 0.3g Cerium)

The microstructure consists of strip like, distributed along the grain boundaries while some granular phases were also found in the inner grains. Neither micro porosities nor stringers were observed.

The tensile and compression tests were carried out using Universal Testing Machine (Model No. MCS/UTE-20T). Tests were carried out on three different test samples of varying composition of Al2024 and Cerium and the results were obtained as follows.

The test samples are indicated in the table and in the graphs as Trail No-1, Train No-2, Trail No-3 as 1920g Al2024 +0.1 g Cerium, 1940g Al2024 + 0.2g Cerium, 1960g Al2024 + 0.3g Cerium respectively. Additionally, things are indicated as follows in the tables.

- *Test Sample: 1920g Al2024 + 0.1g Cerium*

In order to analyse the tensile strength for different dimensions, the specimens were prepared with different dimensions. The specimens used for tensile tests were of the of cylindrical shape and the initial diameters of these three specimens were 13mm, 12.7mm and 12.4mm. The original gauge length of these three specimens was kept constant to 50mm.

- *Tensile Test Results: -*

Table 2 The Cross-Sectional Area of the Trail-1 Tensile Composition is 132.733mm^2

Input Data	Results
Specimen type - round	Ultimate load 18.040 KN
Initial diameter -13 mm	Ultimate tensile strength 135.915 MPa
Final diameter - 0 mm	Elongation 2.180 %
C/S area 132.733 mm^2	Yield load 17.240 KN
Original gauge length 50 mm	Yield stress 129.888 MPa
Final gauge length 51.09 mm	

Table 3 The Cross-Sectional Area of the Trail-1 Tensile Composition is 126.677mm^2

Input Data	Results
Specimen type round	Ultimate load 17.000 KN
Initial diameter 12.7 mm	Ultimate tensile strength 134.916 MPa
Final diameter 0 mm	Elongation 1.400 %
C/S area 126.677 mm^2	Yield load 15.460 KN
Original gauge length 50 mm	Yield stress 122.040 MPa
Final gauge length 50.7 mm	

Table 4 The Cross-Sectional Area of the Trail-1 Tensile Composition is 120.763mm^2

Input Data	Results
Specimen type round	Ultimate load 17.920 KN
Initial diameter 12.4 mm	Ultimate tensile strength 148.394 MPa
Final diameter 0 mm	Elongation 1.600 %
C/S area 120.763 mm^2	Yield load 16.660 KN
Original gauge length 50 mm	Yield stress 137.960 MPa
Final gauge length 50.8 mm	

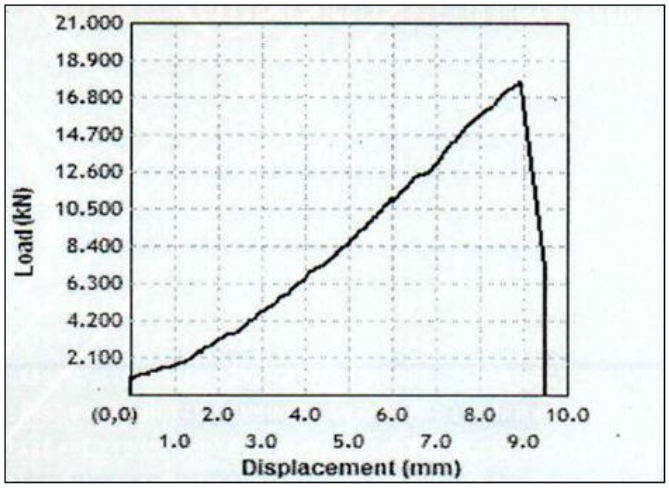

Fig 6 Displacement Variation with Increased Load with Tensile Composition trial-1 is 132.733mm^2.

ISSN No:-2456-2165

The figure 6 portraits the mentioned information about load Vs displacement.A tensile test for Al2024-Cerium is indicated by the load-displacement curve. The curve is initially linear, which shows deformation of the elastics. A major increase indicates that the plastic deformation process is beginning in 1 kN. The curve is elevated by 17 kN, indicating the cessation of deformation and a downwards movement which could be indicative of structural failure or fracture.

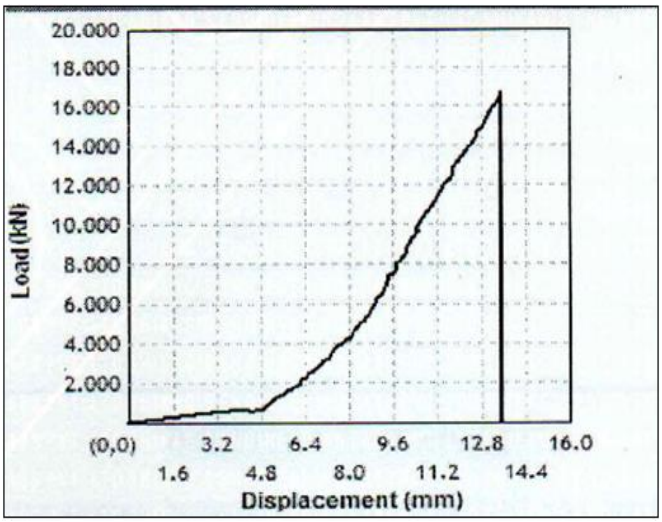

Fig 7 Displacement Variation with Increased Load with Tensile Composition Trial-1 is 126.677mm^2

Initially exhibiting gradual upward progression, the curve represents elastic deformation. At around 4.8 mm displacement, a sudden rise is observed, corresponding to a load increase of 1.5 kN. The subsequent range up to 17 kN signifies the material approaching its yield point, wherein the molecules experience yielding and the load-displacement relationship shifts, eventually leading to a drop in load.

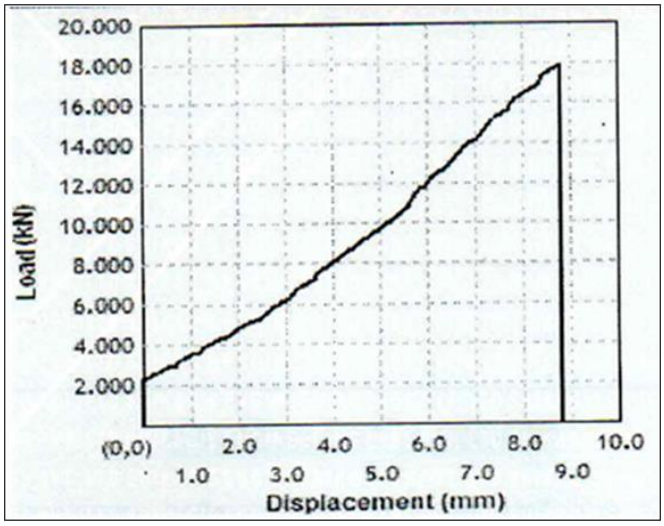

Fig 8 Displacement Variation with Increased Load with Tensile Composition trial-1 is 120.763mm^2

The figure 8 shows how a material responds to being pulled. At first, as more force is applied (up to 18 kN), the material stretches more (displacement increases) following a rule. But beyond 18 kN, the material's arrangement starts breaking down, causing it to stretch less, leading to a decrease in displacement. This shift in behaviour is due to the material struggling to handle the force, and it's seen on the graph where the line goes down.

➢ *Compression Test Results: -*

The specimens used for compression tests were of the of cylindrical shape and the initial diameters of these three specimens were approximately 20mm each (20.94mm, 20.94mm and 19.99mm).

Table 5 Compression Test Results for Trail-1 with an Initial Diameter of 20.94 mm

Input Data	Results
Specimen type round	Ultimate load 200.000 KN
Initial diameter 20.94 mm	Compressive strength 580.745 MPa
Final diameter 0 mm	
C/S area 344.385 mm^2	
Original gauge length 0 mm	
Final gauge length 0 mm	

Table 6 Compression Test Results for Trail-1 with an Initial Diameter of 20.94mm

Input Data	Results
Specimen type round	Ultimate load 201.080 KN
Initial diameter 20.94 mm	Compressive strength 583.873 MPa
Final diameter 24.3 mm	
C/S area 344.385 mm^2	
Original gauge length 0 mm	
Final gauge length 0 mm	

Table 7 Compression Test Results for Trail-1 with an Initial Diameter of 19.99mm

Input Data	Results
Specimen type round	Ultimate load 173.980 KN
Initial diameter 19.99 mm	Compressive strength 554.341 MPa
Final diameter 24.85 mm	
C/S area 313.846 mm^2	
Original gauge length 0 mm	
Final gauge length 0 mm	

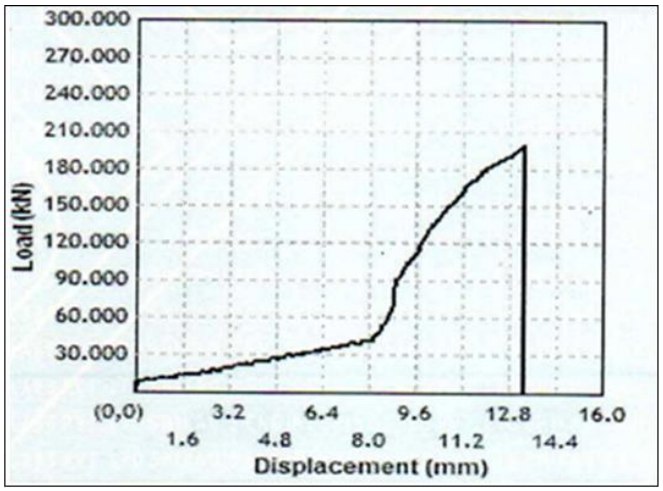

Fig 9 Displacement Variation with Increased Load with Compression Composition Trial-1 is 20.94mm

ISSN No:-2456-2165

This figure 9 illustrates the load-displacement relationship for Al2024-cerium material. Initially, load increases proportionally wih displacement.Aroung 50kN, a curve emerges indicating altered behaviour notably beyond 200kN load. This trend shifts in the materials mechanical properties and behaviour as load and displacement increase.

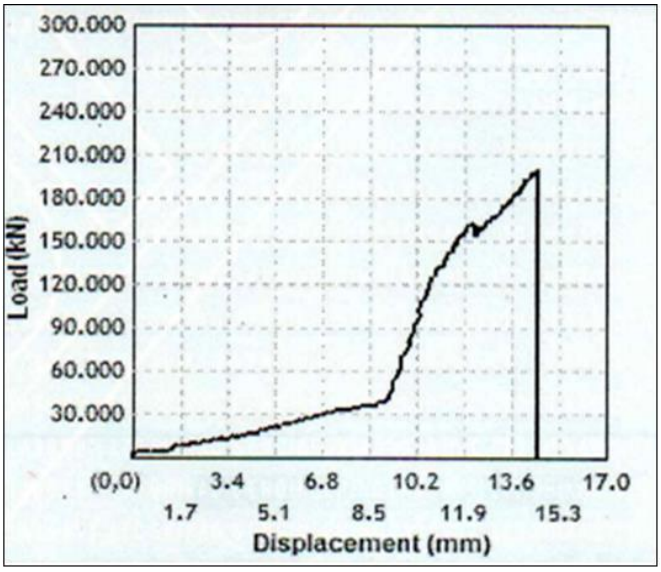

Fig 10 Displacement Variation with Increased Load with Compression Composition Trial-1 20.94mm

This figure 10 portrays the load-displacement characteristics of Al2024-cerium material. Upon applying a load of 5kN and incrementing displacement to 1.7mm, an initial linear relationship is observed. However, at 50kN load, the curve emerges, indicating potential plastic deformation or a shift in the material's elastic behaviour. The curve ascends up to 160kN, displaying a region of increased stiffness, after which a slight drop of 150kN, possibly due to stress relaxation. The subsequent rise to 200kN is met with a sudden load drop, indicative of a critical failure point, suggesting possible buckling or material fracture.

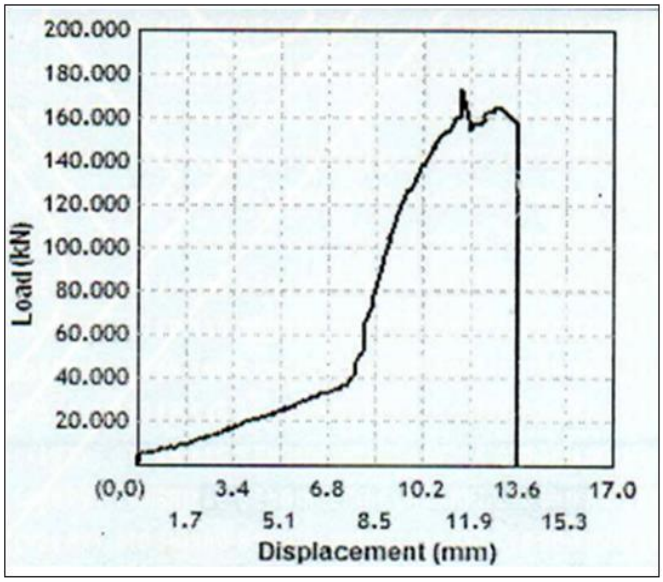

Fig 11 Displacement Variation with Increased Load with Compression Composition Trial-1 19.99mm

The above Figure 11 shows the information upon applying a load of 5kN and incrementing displacement to 1.7mm, an initial linear relationship is observed. However, at 50kN load, the curve emerges, indicating potential plastic deformation or a shift in the material's elastic behaviour. The curve ascends up to 160kN, displaying a region of increased stiffness, after which a slight drop of 150kN, possibly due to stress relaxation. The subsequent rise to 200kN is met with a sudden load drop, indicative of a critical failure point, suggesting possible buckling or material fracture.

➢ *Brinell Hardness Test: -*

Brinell hardness test is performed using Rockwell Cum Brinell Hardness machine. Hardness is property of material to withstand the localised plastic deformation. The Brinell hardness test is performed to determine the Brinell Hardness number of the test specimen. The Brinell hardness number represents the harness level of the specimen.

Table 8 Hardness Test Results of Trail-1 Test Sample

Sl. No.	Material	Observed Impression Values in HB			
		1.	2.	3.	Average
1.	1940g Al2024 + 0.1g Cerium	101	101	99.5	100.50
2.	1940g Al2024 + 0.1g Cerium	102	102	101	101.67
3.	1940g Al2024 + 0.1g Cerium	98.3	98.3	99.5	98.70

- *Test Sample: 1940g Al2024 + 0.2g Cerium*

In order to analyse the tensile strength for different dimensions, the specimens were prepared with different dimensions. The specimens used for tensile tests were of the of cylindrical shape and the initial diameters of these three specimens were 12.75mm, 12.3mm and 12.65mm.

➢ *Tensile Test Results: -*

Table 9 The Cross-Sectional Area of the Trail-2 Tensile composition is 127.75mm^2

Input Data	Results
Specimen type round	Ultimate load 12.980 KN
Initial diameter 12.75 mm	Ultimate tensile strength 101.660 Mpa
Final diameter 0 mm	Elongation 3.720 %
C/S area 127.677 mm^2	Yield load 7.240 KN
Original gauge length 50 mm	Yield stress 56.704 Mpa
Final gauge length 51.86 mm	

Table 10 The Cross-Sectional Area of the Trail-2 Tensile Composition is 118.823mm^2

Input Data	Results
Specimen type round	Ultimate load 4.660 KN
Initial diameter 12.3 mm	Ultimate tensile strength 39.219 Mpa
Final diameter 0 mm	Elongation 2.720 %
C/S area 118.823 mm^2	Yield load 3.660 KN
Original gauge length 50 mm	Yield stress 30.803 Mpa
Final gauge length 51.36 mm	

ISSN No:-2456-2165

Table 11 The Cross-Sectional Area of the Trail -2 Tensile Composition is 125.682mm^2

Input Data	Results
Specimen type round	Ultimate load 11.140 KN
Initial diameter 12.65 mm	Ultimate tensile strength 88.638 MPa
Final diameter 0 mm	Elongation 3.600 %
C/S area 125.682 mm^2	Yield load 10.620 KN
Original gauge length 50 mm	Yield stress 84.500 MPa
Final gauge length 51.8 mm	

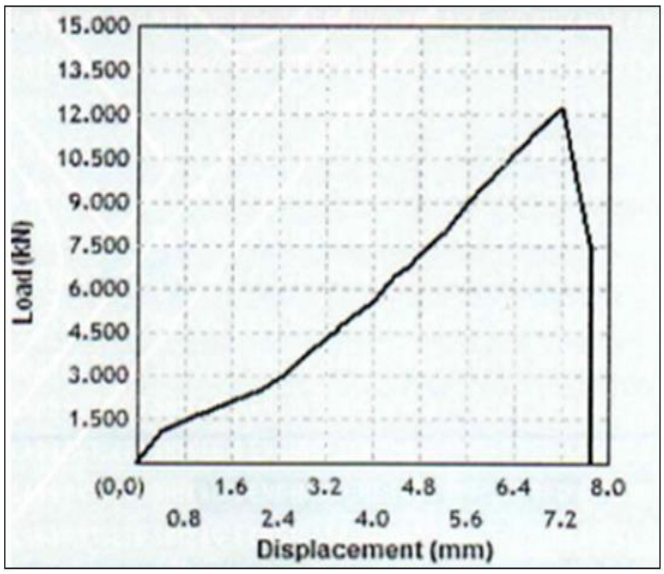

Fig 12 Variation of Displacement with Increase in Load (kN) of Tensile Composition for Trial-2 is 12.75mm

The figure 12 shows mentioned trial -2 upon an initial displacement increase to 0.5 mm, load rises steadily. At 7.2 mm displacement, a significant increase in load to 12000 kN is observed, likely indicating material yielding or plastic deformation. Beyond this point, load rises sharply up to 1500 kN, maintaining a linear trend, possibly reflecting elastic deformation. However, load decreases at 7500 kN, suggesting potential material failure or structural instability.

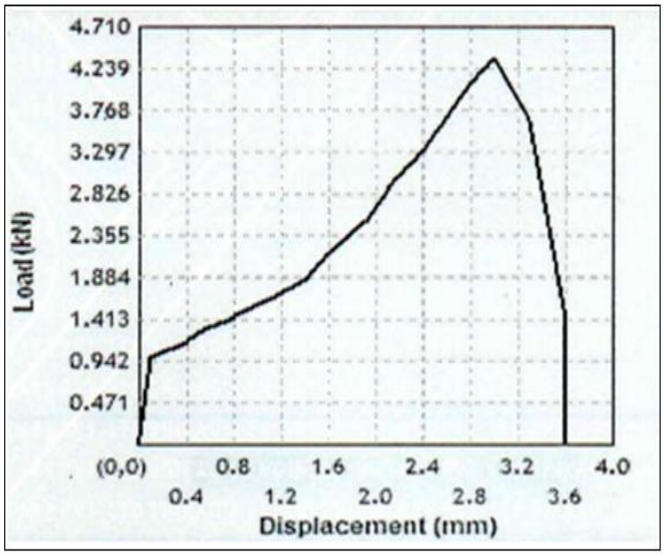

Fig 13 Variation of Displacement with Increase in Load (kN) of Tensile Composition for Trail-2 is 12.3mm

The figure 13 illustrates the relationship between displacement and load, where the curve starts linearly, representing elastic deformation. At 0.942 mm, displacement sharply rises to 3.0 mm due to applied force. As load decreases at 4.240 kN, it indicates potential plastic deformation or failure in the composite material. These observations provide insights into the mechanical behaviour of the AL2024-Cerium composite under tension.

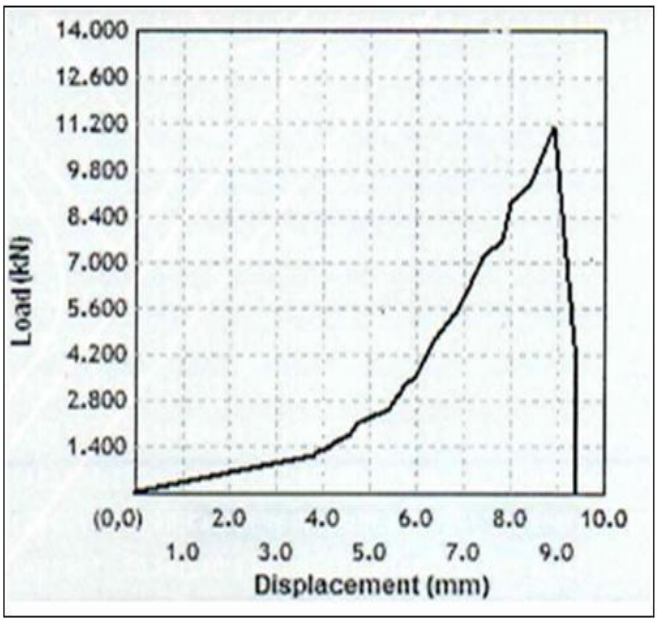

Fig 14 Variation of Displacement with Increase of Load (KN) of Tensile Composition for Trail-2 is 12.65mm

The figure 14 shows how a material responds to being pulled. At first, as more force is applied (up to 18 kN), the material stretches more (displacement increases) following a rule. But beyond 18 kN, the material's arrangement starts breaking down, causing it to stretch less, leading to a decrease in displacement. This shift in behavior is due to the material struggling to handle the force, and it's seen on the graph where the line goes down.

- *Compression Test Results: -*

The specimens used for compression tests were of the of cylindrical shape and the initial diameters of these three specimens were 19mm, 21mm and 21.09mm.

Table 12 Compression Test Results for Trail-2 with an Initial Diameter of 19mm.

Input Data	Results
Specimen type round	Ultimate load 173.440 KN
Initial diameter 19. mm	Compressive strength 611.717 MPa
Final diameter 23.96 mm	
C/S area 283.529 mm2	
Original gauge length 0 mm	
Final gauge length 0 mm	

ISSN No:-2456-2165

Table 13 Compression Test Results for Trail-2 with an Initial Diameter of 21mm

Input Data	Results
Specimen type round	Ultimate load 202.860 KN
Initial diameter 21 mm	Compressive strength 585.691 MPa
Final diameter 23.7 mm	
C/S area 346.361 mm2	
Original gauge length 0 mm	
Final gauge length 0 mm	

Table 14 Compression Test Results for Trail-2 with an Initial Diameter of 21.09mm

Input Data	Results
Specimen type round	Ultimate load 200.340 KN
Initial diameter 21.09 mm	Compressive strength 573.481 MPa
Final diameter 0 mm	
C/S area 349.337 mm^2	
Original gauge length 0 mm	
Final gauge length 0 mm	

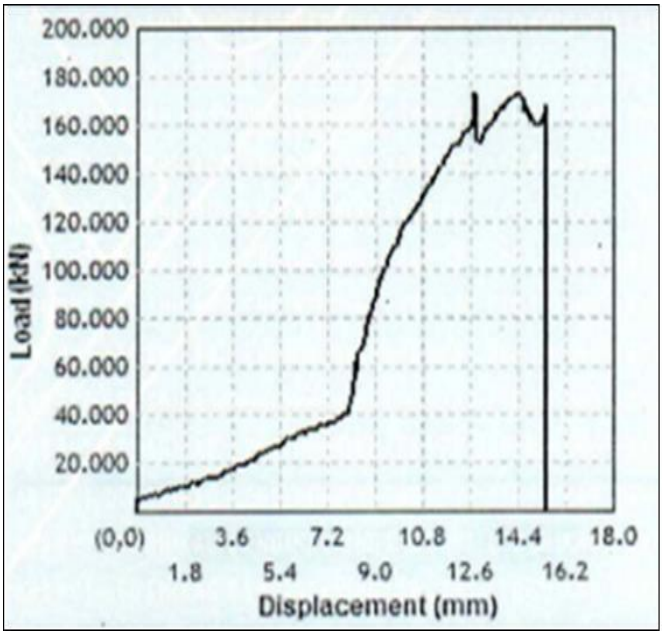

Fig 15 Displacement Variation with Increased Load with Compression Composition Trial-2 is 19mm

Initially, the curve indicates elastic deformation, as load increases with minimal displacement. At 40 kN, a noticeable curve initiates, suggesting a transition. Deformation is significant at 170 kN, causing a curve decline. The curve rises, peaking around 180 kN, before decreasing again. At 165 kN, there's a brief upward turn, followed by a decline. Finally, at 16.2 mm displacement, the curve descends. The graph demonstrates the material's intricate response to varying loads, implying possible yielding, plasticity, and possibly fracture.

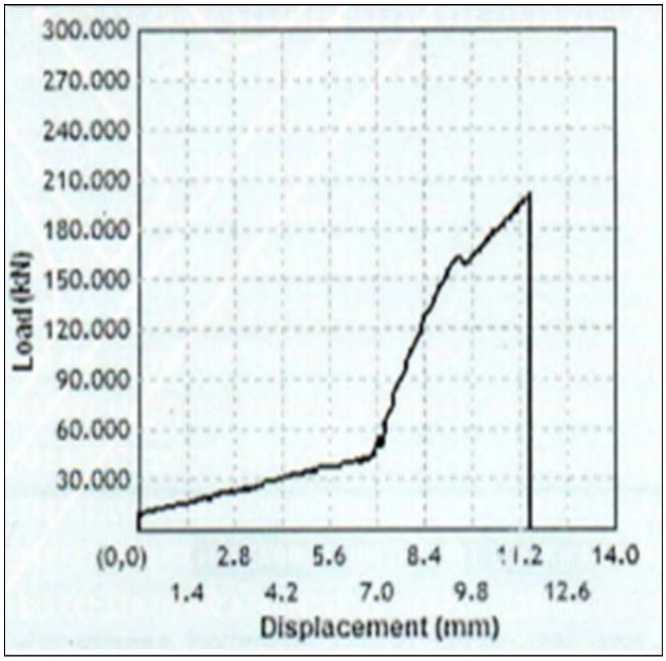

Fig 16 Displacement Variation with Increased Load with Compression Composition Trial-2 is 21mm.

The figure 16 depicts load against displacement. Initially, the curve rises from 10 kN to 7 mm displacement. Afterward, a gradual curve indicates slight elastic deformation. At 9.8 mm, yielding commences, coinciding with load increase up to 170 kN, suggesting material alteration. This behaviour highlights the interplay of load and displacement, showcasing a potential yield point where the material's response changes due to underlying properties and structural changes.

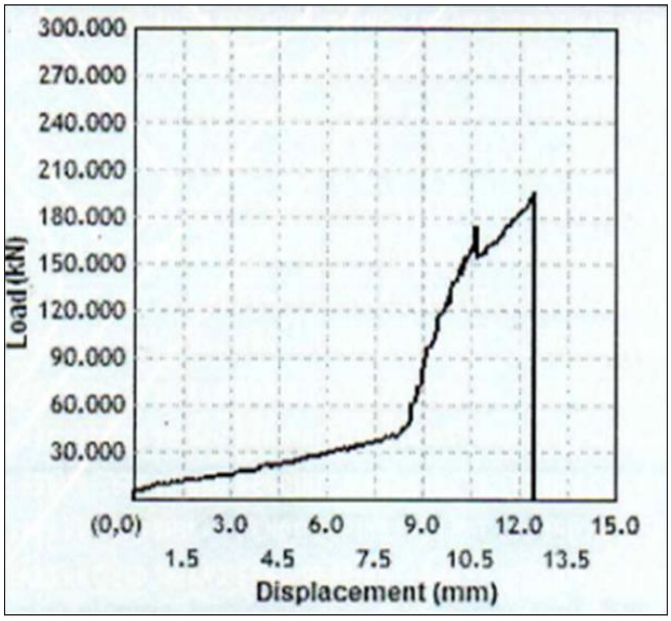

Fig 17 Displacement Variation with Increased Load (KN) with Compression Composition Trial-2 is 21.09mm

ISSN No:-2456-2165

The figure 17 depicts load against displacement. Initially, the curve rises from 10 kN to 7 mm displacement. Afterward, a gradual curve indicates slight elastic deformation. At 9.8 mm, yielding commences, coinciding with load increase up to 170 kN, suggesting material alteration. This behaviour highlights the interplay of load and displacement, showcasing a potential yield point where the material's response changes due to underlying properties and structural changes.

➢ *Brinell Hardness Test:-*

Brinell hardness test is performed using Rockwell Cum Brinell Hardness machine. Hardness is property of material to withstand the localised plastic deformation. The Brinell hardness test is performed to determine the Brinell Hardness number of the test specimen. The Brinell hardness number represents the harness level of the specimen.

Table 15 Hardness Test Results of Trail-2 Test Samples

Sl. No.	Material	Observed Impression Values in HB			
		1	2	3	Average
1.	1940g Al2024 + 0.2g Cerium	103	103	102	102.67
2.	1940g Al2024 + 0.2g Cerium	103	103	104	103.33
3.	1940g Al2024 + 0.2g Cerium	101	101	102	101.33

- *Test Sample: 1960g Al2024 + 0.3g Cerium*

➢ *Tensile Test Results: -*

In order to analyse the tensile strength for different dimensions, the specimens were prepared with different dimensions. The specimens used for tensile tests were of the of cylindrical shape and the initial diameters of these three specimens were 12.74mm, 12.9mm and 12.93mm.

Table 16 The Cross-Sectional Area of the Trial-3 Tensile Composition is 127.746mm2

Input Data	results
Specimen type round	Ultimate load 3.800 KN
Initial diameter 12.74 mm	Ultimate tensile strength 29.809 MPa
Final diameter 0 mm	Elongation 1.800 %
C/S area 127.476 mm^2	Yield load 1.360 KN
Original gauge length 50 mm	Yield stress 10.668 MPa
Final gauge length 51.9 mm	

Table 17 The Cross-Sectional Area of the Trail-3 Tensile Composition is 130.698mm2

Input Data	Results
Specimen type round	Ultimate load 14.420 KN
Initial diameter 12.9 mm	Ultimate tensile strength 110.329 MPa
Final diameter 0 mm	Elongation 1.720 %
C/S area 130.698 mm^2	Yield load 12.060 KN
Original gauge length 50 mm	Yield stress 92.272 MPa
Final gauge length 50.86 mm	

Table 18 The Cross-Sectional Area of the Trial-3 Tensile Composition is 131.307mm^2

Input Data	Results
Specimen type round	Ultimate load 11.200 KN
Initial diameter 12.93 mm	Ultimate tensile strength 85.294 MPa
Final diameter 0 mm	Elongation 3.400 %
C/S area 131.307 mm^2	Yield load 10.680 KN
Original gauge length 50 mm	Yield stress 81.334 MPa
Final gauge length 51.7 mm	

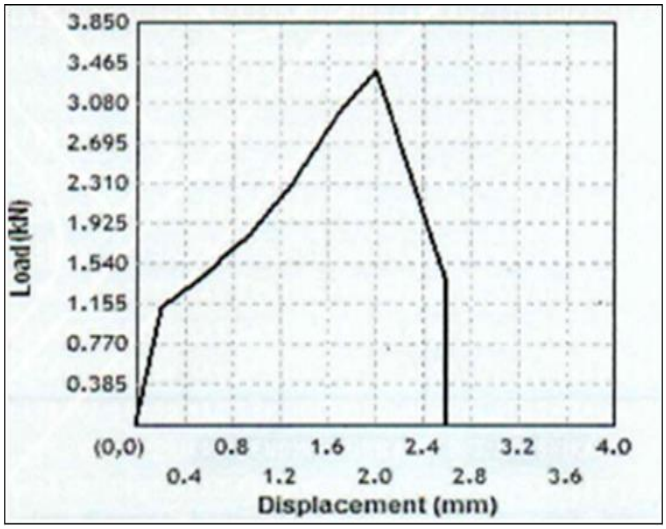

Fig 18 Displacement Variation with Increased Load with Tensile Composition Trial-3 is 12.74mm

The figure 18 represents load versus displacement. With an x-axis variation of 0.4mm and y-axis variation of 0.385kN, the graph initially shows elastic deformation. As load increases, displacement rises, particularly at 0.2mm. From 1.155kN, displacement remains consistent until 2mm, resembling a straight line. Load increases to 3.080kN, then gradually returns. This behaviour, observed until 2.6mm displacement, reflects the material's response to varying loads, showcasing elastic properties, stability, and the influence of external forces.

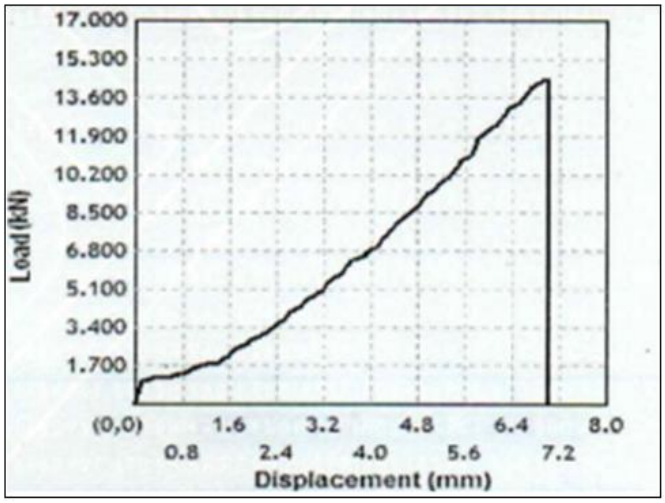

Fig 19 Displacement Variation with Increased Load with Tensile Composition Trial-3 is 12.9mm

ISSN No:-2456-2165

In the provided figure 19, the changes in load and displacement occur due to the material's molecular arrangement. The load variation begins around 1.5 kN, leading to a gradual increase in displacement as the material's molecules are slightly compacted. However, at approximately 7.1 mm displacement, a drop signifies a change in the material's deformation behaviour. This change could be attributed to alterations in the material's internal structure, affecting its mechanical response under load.

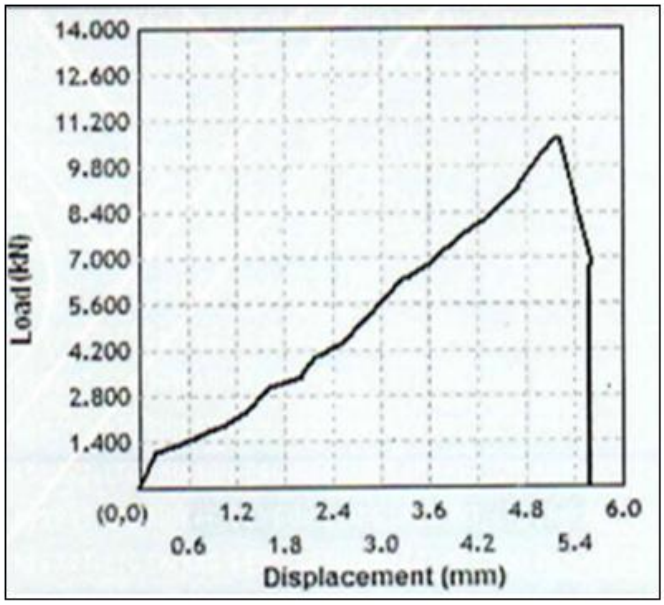

Fig 20 Displacement Variation with Increased Load with Tensile Composition Trial-3 is 12.93mm

The figure 20 indicates an increase in load at 1.4 kN with an x-axis variation of 0.6 mm. The material's composition, potentially containing yttrium, results in tightly packed molecules. As the load increases, the graph rises relative to displacement. Around 10 kN, the load reaches an approximate value, after which the graph experiences a downward shift at a displacement of 5.6 mm. This behaviour could reflect the material's response to applied forces, influenced by its composition and structural characteristics.

- *Compression Test Results: -*

The specimens used for compression tests were of the of cylindrical shape and the initial diameters of these three specimens were 21.08mm, 20.5mm and 21.13mm.

Table 19 Compression Test Results for Trail-3 with an Initial Diameter of 21.08mm.

Input Data	Results
Specimen type round	Ultimate load 200.340 KN
Initial diameter 21.08 mm	Compressive strength 574.024 MPa
Final diameter 25.2 mm	
C/S area 349.005 mm2	
Original gauge length 0 mm	
Final gauge length 0 mm	

Table 20 Compression Test Results for Tail-3 with an Initial Diameter of 20.05mm

Input Data	Results
Specimen type round	Ultimate load 200.000 KN
Initial diameter 20.5 mm	Compressive strength 605.950 MPa
Final diameter 23.79 mm	
C/S area 330.064 mm2	
Original gauge length 0 mm	
Final gauge length 0 mm	

Table 21 Compression Test Results for Trail-3 with an Initial Diameter of 21.13mm

Input Data	Results
Specimen type round	Ultimate load 200.000 KN
Initial diameter 21.13 mm	Compressive strength 570.353 MPa
Final diameter 24.54 mm	
C/S area 350.663 mm2	
Original gauge length 0 mm	
Final gauge length 0 mm	

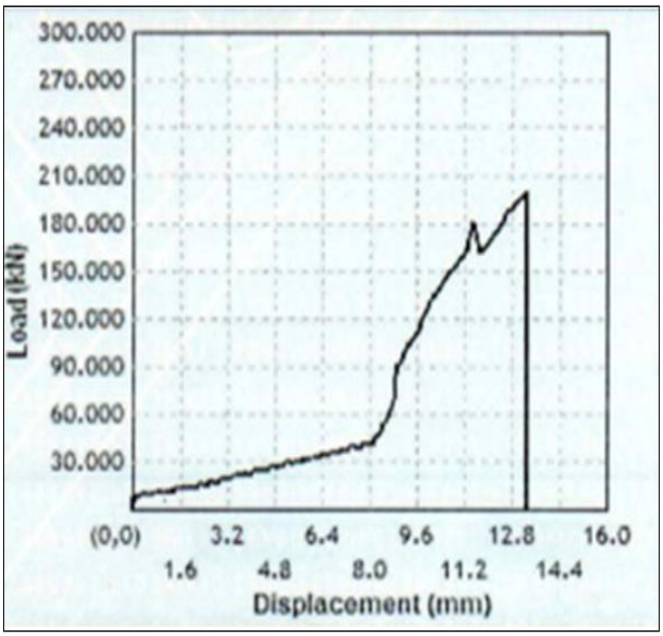

Fig 21 Displacement Variation with Increased Load with Compression Composition is 21.08mm

The figure 21 illustrates load versus displacement, with an x-axis variation of 1.6mm and y-axis variation of 30kN. Initially, the curve rises gradually from a lower load to around 20kN as displacement increases. Then, a curvature forms, indicating elastic deformation. Load continues to increase in relation to displacement until 11.2mm, where it reaches its highest value at approximately 200kN. Afterward, load decreases to around 140kN, followed by another increase and decrease. This pattern likely signifies complex material behaviour under varying loads, potentially involving yielding, plastic deformation, or structural changes due to external forces.

ISSN No:-2456-2165

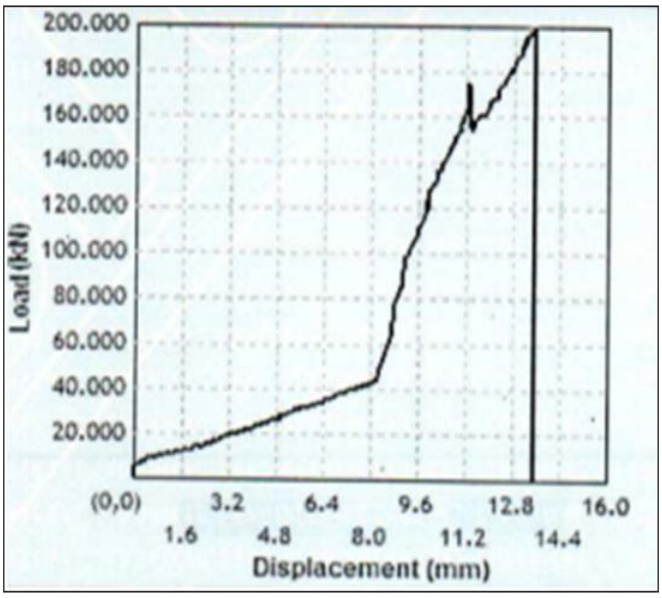

Fig 22 Displacement Variation with Increased Load (KN) with Compression Composition Trial-3 is 20.5mm

The figure 22 portrays the relationship between load and displacement. Initially, the graph remains linear, representing elastic deformation. A curve subsequently develops, signifying a change in behaviour. Following this curve, the graph maintains a straight trend up to 170 kN. Then, there is a noticeable drop, followed by a rise to 200 kN and another decrease. These variations indicate shifts in the material's mechanical response, structural changes due to external forces.

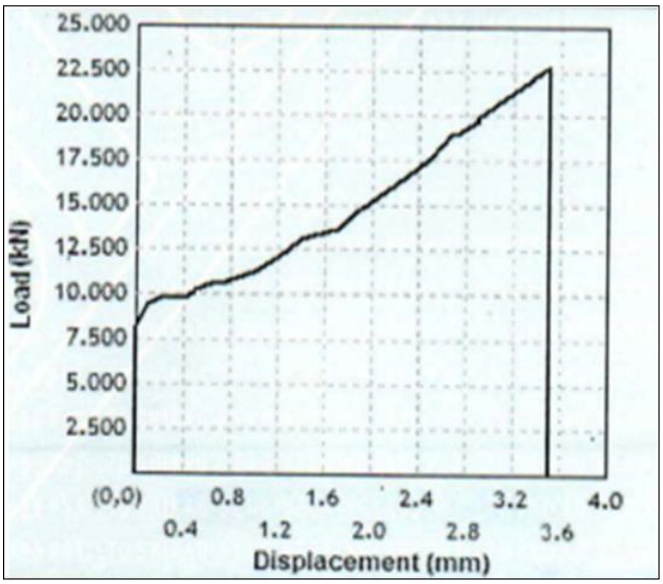

Fig 23 Displacement Variation with Increased Load (KN) Compression Composition Trial-3 is 21.13mm

The figure 23 demonstrates load against displacement, with a small x-axis variation of 0.4mm and y-axis variation of 2.5kN. Starting at 7.5kN, the graph exhibits a gradual increase followed by slight oscillations. Reaching around 21kN, the load peaks, leading to a minor decrease. This pattern may suggest material instability or localized effects impacting its response to increasing loads.

- *Brinell Hardness Test: -*

Brinell hardness test is performed using Rockwell Cum Brinell Hardness machine. Hardness is property of material to withstand the localised plastic deformation. The Brinell hardness test is performed to determine the Brinell Hardness number of the test specimen. The Brinell hardness number represents the harness level of the specimen.

Table 22 Hardness Test Results of Trial-3 Test Sample

Sl. No.	Material	Observed Impression Values in HB			
		1	2	3	Average
1.	1940g Al2024 + 0.3g Cerium	108	107	108	107.67
2.	1940g Al2024 + 0.3g Cerium	108	110	110	109.33
3.	1940g Al2024 + 0.3g Cerium	111	110	110	110.33

IV. CONCLUSION

From the results obtained from the experiments, it is concluded that the use of very small amount of rare earth metal (Cerium) will enhance the chemical properties and the physical properties too. The reinforcement of Aluminium 2024 with cerium particles increased the hardness of the test specimen (Al2024 + Cerium), also it concludes that the increase in the quantity of cerium increases the hardness of the specimen.

FUTURE WORKS

From the current experiments it is observed that the addition of small amounts of cerium to aluminum has increased alloy tolerances to impurities such as Cu and Fe and improved overall corrosion resistance. Every beginning has an end and every end has a new beginning, likewise this is not the final stage, but it is the infant stage of the concept of reinforcement of rare metals with aluminum alloys. Further still more experiments will be carried out to stand nearby the accuracy of the results and the clarity regarding the chemical properties and physical properties. Also, it has a bright futuristic application in the upcoming days.

REFERENCES

[1]. Surface & Coatings Technology http://dx.doi.org/ 10.1016/j.surfcoat.2017.06.088 The mechanical and tribological properties of Ti [Nb, V] N films on the Al2024 alloy Özlem Barana, Ayşenur Keleş, Hikmet Çiçek, Yaşar Totik, İhsan Efeoğlu

[2]. International Journal of Adhesion and Adhesives https://doi.org/10.1016/j.ijadhadh.2019.102433 Polybenzimidazole adhesive bonded aluminum-2024 joints for structural applications Muhammad Faisal Shahzada, M.P. Mughal, H.M.S. Iqbal, N.A. Mufti, M.Q. Saleem

[3]. Surfaces and Interfaces https://doi.org/10.1016/ j.surfin.2019.02.005 Achieving non-adsorptive anodized film on Al-2024 alloy: Surface and electrochemical corrosion investigation M. Faizan Khana, A. Madhan Kumar, Anwar Ul-Hamid, Luai M. Al-Hems
[4]. Material Research Express https://doi.org/ 10.1088/2053-1591/ab2ee1 Comparison of wear properties of HVOF sprayed WC-Co and WC-CoCr coatings on Al alloys H Varol Özkavak, Ş Şahin, M F Saraç and Z Alkan
[5]. Arabian Journal for Science and Engineering https://doi.org/10.1007/s13369-019-03924-5 Improvement of Mechanical Properties of 2024 AA by Reinforcing Yttrium and Processing Through Spark Plasma Sintering Ch. S. Vidyasagar, and D. Benny Karunakar
[6]. The International Journal of Advanced Manufacturing Technology (2020) 108:1173–1187 https://doi.org/ 10.1007/s00170-020-05228-7 Experimental analysis and characterization of SiC and RE oxides reinforced Al-6063 alloy-based hybrid composites Vipin Kumar Sharma, Vinod Kumar, Ravinder Singh Joshi and Deepak Sharma
[7]. Metals and Materials International https://doi.org/ 10.1007/s12540-020-00727-4 Efects of Nano yttrium and Spark Plasma Sintering on the Mechanical Properties of AA2024 Matrix Composites C. H. Suresh Vidyasagar, D. Benny Karunakar
[8]. Progress in Natural Science: Materials International https://doi.org/10.1016/j.pnsc.2021.07.001 Effect of spark plasma sintering and reinforcements on the formation of ultra-fine and nanograins in AA2024-TiB2-Y hybrid composites CH. Suresh Vidyasagar, D.B. Karunakar.
[9]. Silicon (2022) 14:4009–4026 https://doi.org/ 10.1007/s12633-021-01158-5 Experimental Investigation and Optimization of Dry Sliding Wear Test Parameters of Aluminum Based Composites Mohammad Mohsin Khan, Abhijit Dey. Mohammad Irfan Hajam.
[10]. Sharma, S.C., (1997). Mechanical. properties and fractography of cast lead / quartz particulate composites, materials and design, vol-18, 149-153
[11]. Kok, M., (2005). Production and mechanical properties of Al2O3 particle reinforced 2024 aluminium alloy composites, journal of materials processing technology, 381-387
[12]. Kataiah, G. S., (2010). The mechanical properties and fractography of aluminium 6061-TiO2 composites, international journal of pharmaceutical studies and research, vol-1, 17-25
[13]. Seah, K. H. W., Sharma, S. C. and Girish, B. M., (1997). Mechanical properties of as-cast and heat-treated ZA-27/graphite particulate composites, Composites Part A, 28A, 251-256
[14]. Cuvalc, H., Bas, H., (2004). Investigation of the tribological properties of silicon containing zinc–aluminum based journal bearings, Tribology International, 37, 433–440
[15]. Badisch, E., Ilo, S., Polak, R., (2009). Multivariable Modeling of ImpactAbrasion Wear Rates in Metal Matrix-Carbide Composite Materials, Tribol Lett 36:55–62
[16]. Seenappa & Sharma, K.V., (2011). Characterization of Mechanical and Micro structural properties of ZA alloys, International Journal of Engineering Science and Technology (IJEST), Vol. 3 No. 3
[17]. Modi, O. P., Rathod, S., Prasad, B. K., Jha, A. K., and Dixit, G., (2007). The influence of alumina article dispersion and test parameters on dry sliding wear behavior of Zinc-based alloy, Tribology Internationnal, 40, 1137-1146
[18]. Dominguez, C., Lopez, M. V. M., Ri´os-jara, D., (2002). The influence of manganese on the microstructure and the strength of a ZA-27 alloy, Journal of Materials Science, 37, 5123 – 5127
[19]. Ranganath, G., Sharma, S.C., Krishna, M., and Muruli, M.S., (2002). A Study of Mechanical Properties and Fractography of ZA-27/Titanium-Dioxide Metal Matrix Composites. Journal of Materials Engineering and Performance;11(4): 408-13
[20]. Sharma, S. C., Girish, B. M., Somashekar, D. R., Kamath, R., Satish, B. M., (1999). Mechanical Properties and fractography of Zircon-particle-reinforced ZA-27 alloy composite materials, Composites science and technology, 59, 1805- 1812
[21]. Chen, T., Yuan, C., Fu, M., Ma, Y., Li, Y. and Hao, Y., (2009). Friction and wear properties of casting in-situ silicon particle reinforced ZA27 composites, China Foundry, Vol.6 No.1, 1-8
[22]. Chen, T. J., Yuan, C. R., Fu, M. F., Ma, Y., Li, Y. D., Hao, Y., (2008). In-situ silicon particle reinforced ZA27 composites. Part I: microstructures and tensile properties. Materials Science Technology, 24: 1321-1332
[23]. Bobic, I., Jovanovic, M.T., Ilic, N., (2003). Microstructure and Strength of ZA27-based composites reinforced with Al2O3 particle, Materials Letters, 57, 1683- 88